Virology 481 (2015) 51–62

Contents lists available at ScienceDirect

Virology

journal homepage: www.elsevier.com/locate/yviro

Porcine reproductive and respiratory syndrome virus nonstructural protein 2 (nsp2) topology and selective isoform integration in artificial membranes ☆

Matthew A. Kappes [a,b], Cathy L. Miller [b], Kay S. Faaberg [a,*]

[a] Virus and Prion Research Unit, USDA-ARS-National Animal Disease Center, Ames, IA, USA
[b] Department of Veterinary Microbiology and Preventive Medicine, College of Veterinary Medicine, Iowa State University, Ames, IA, USA

ARTICLE INFO

Article history:
Received 6 December 2014
Returned to author for revisions
15 January 2015
Accepted 30 January 2015
Available online 11 March 2015

Keywords:
Porcine reproductive and respiratory syndrome virus
Arterivirus
Nonstructural protein 2
Membrane topology
Structural protein
Protein isomers

ABSTRACT

The membrane insertion and topology of nonstructural protein 2 (nsp2) of porcine reproductive and respiratory syndrome virus (PRRSV) strain VR-2332 was assessed using a cell free translation system in the presence or absence of artificial membranes. Expression of PRRSV nsp2 in the absence of all other viral factors resulted in the genesis of both full-length nsp2 as well as a select number of C-terminal nsp2 isoforms. Addition of membranes to the translation stabilized the translation reaction, resulting in predominantly full-length nsp2 as assessed by immunoprecipitation. Analysis further showed full-length nsp2 strongly associates with membranes, along with two additional large nsp2 isoforms. Membrane integration of full-length nsp2 was confirmed through high-speed density fractionation, protection from protease digestion, and immunoprecipitation. The results demonstrated that nsp2 integrated into the membranes with an unexpected topology, where the amino (N)-terminal (cytoplasmic) and C-terminal (luminal) domains were orientated on opposite sides of the membrane surface.

Published by Elsevier Inc.

Introduction

Viruses are obligate intracellular pathogens that modulate the host cellular environment to establish locations conducive to the biogenesis of infectious progeny. Positive-sense RNA viruses modify host cellular membranes of intracellular compartments including mitochondria (Gant et al., 2014; Miller et al., 2001), chloroplasts (Wei et al., 2010), endoplasmic reticulum (ER)/Golgi (Delgui et al., 2013; Gillespie et al., 2010; Hsu et al., 2010; Wei et al., 2010), and endosomes/lysosomes (Magliano et al., 1998) to establish structured sites of replication (replication complexes (RCs)). Enveloped viruses further require the ability to capture cellular membranes as a component of progeny virions during egress. Porcine reproductive and respiratory syndrome virus (PRRSV) is an enveloped single-stranded positive-sense RNA virus within the *Arteriviridae* family (Baker, 2012). The first approximately three-fourths of the genome encode at least 14 nonstructural proteins (nsp) from a large polyprotein precursor (pp1a/b) which is co-translationally and post-translationally processed by four viral proteases including the papain-like cysteine proteinase 1α (PLP1α; nsp1α), PLP1β (nsp1β), PLP2 (nsp2), and the main serine proteinase (SP; nsp4) (Fig. 1) (Fang and Snijder, 2010). The final one-fourth of the genome encodes nine additional ORFs, including all canonical structural proteins (Snijder et al., 2013). Of the replicase proteins, nsp2 is unique due to its large size (~1196 amino acids (aa)), genetic heterogeneity, its participation in diverse roles supporting the viral replication cycle, and its packaging within the PRRSV virion (Fang et al., 2012a, 2012b; Kappes et al., 2013; Li et al., 2014; Sun et al., 2012; van Kasteren et al., 2013). The amino (N)-terminal PLP2 protease domain of nsp2 is recognized for its dual functionality between viral pp1a/b processing (Fang and Snijder, 2010; Han et al., 2009) and its immunomodulatory deubiquitinating activity (Deaton et al., 2014; Frias-Staheli et al., 2007; van Kasteren et al., 2012). However, outside of the context of the PLP2 protease domain, very little is known about the potential functional roles for the large central and C-terminal domains of nsp2. The PRRSV nsp2 is a predicted transmembrane protein due to the recognized hydrophobic domain near its C-terminal end (Fig. 1). The arterivirus prototype equine arteritis virus (EAV) nsp2 has been shown to function in membrane rearrangement in support of the formation of double-membrane vesicles (DMVs) RCs (Pedersen et al., 1999; Snijder et al., 2001) and ORF1a polyprotein processing (Han et al., 2009; Wassenaar et al., 1997; Ziebuhr et al., 2000), believed to

☆ Disclaimer: mention of trade names or commercial products in this article is solely for the purpose of providing specific information and does not imply recommendation or endorsement by the U.S. Department of Agriculture.

* Correspondence to: USDA, Agricultural Research Service, Virus and Prion Research Unit, Mailstop 2S-209, National Animal Disease Center, 1920 Dayton Avenue, Ames, IA 50010, USA. Tel.: +1 515 337 7259; fax: +1 515 337 7458.
E-mail address: kay.faaberg@ars.usda.gov (K.S. Faaberg).

http://dx.doi.org/10.1016/j.virol.2015.01.028
0042-6822/Published by Elsevier Inc.

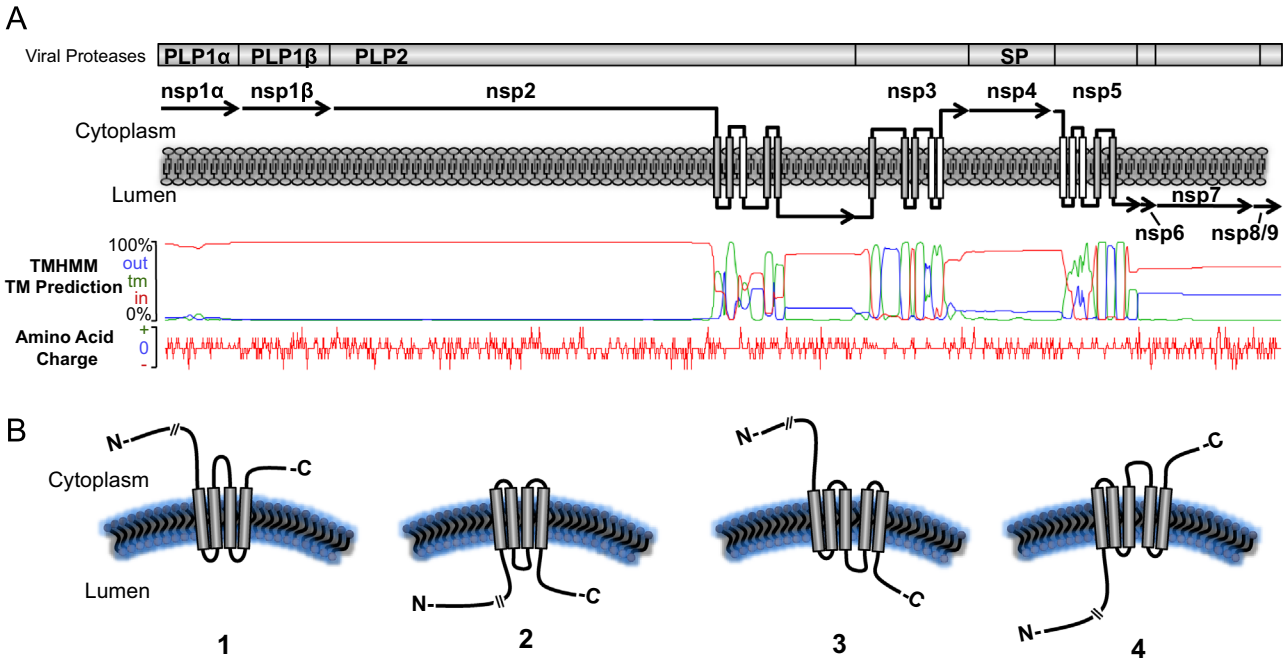

Fig. 1. PRRSV ORF1a encodes putative multi-spanning transmembrane domains. Predicted hydrophobicity of the entire ORF1a coding region is depicted using the TMHMM prediction algorithm within the Geneious software platform. (A) Top: graphical representation of pp1a noting the location of viral protease domains PLP1α, PLP1β, PLP2, SP. Middle: model of membrane integration sites and topologies of pp1a based upon predicted transmembrane spanning helices. Regions where the putative transmembrane spanning domains are unclear are denoted in white. Bottom: plot of hydrophobicity strength scores (TOPCONS) and amino acid charge by position. (B) Possible topologies of nsp2 dependent on even (1 and 2) or odd (3 and 4) number of transmembrane spanning elements and cytoplasmic versus luminal orientation.

be intrinsically associated with ER membrane integration (Knoops et al., 2012). Recently the PRRSV nsp2 was also shown to be packaged within or upon the PRRSV virion, presumably through interaction with the viral envelope (Kappes et al., 2013). While PRRSV nsp2 has been historically recognized as a putative multi-spanning transmembrane protein, the membrane insertion, topology and functionality of the nsp2 hydrophobic domain has never been conclusively determined. In this report, membrane association of full-length nsp2 and sub-dominant isoforms were defined. Full-length nsp2 was further demonstrated to be an integral membrane protein. Nsp2 integration resulted in an unexpected topological orientation within the cell-free in vitro translation system, resulting in a *trans* topology whereas the N-terminus remained cytoplasmic but the C-terminal domain embedded within artificial membranes and maintained a luminal orientation. To our knowledge, this data constitutes the first molecular data defining the PRRSV nsp2 as an integral membrane protein.

Results

Nsp2 expression

Nsp2 was assessed in the absence of all other viral components by use of a rabbit reticulocyte cell-free translation system as outlined in the materials and methods. To assess the genesis and membrane integration of PRRSV nsp2, untagged nsp2 (pNsp2), N-terminal Flag-tagged nsp2 (pNsp2 N-FLAG) or C-terminal Flag-tagged nsp2 (pNsp2 C-FLAG) was assessed both in the absence and presence of microsomal membranes. In all experiments, the non-template control (NTC) and pcDNA vector control (expression plasmid only) reactions were free of any detectable translation products (Fig. 2A – D). General ^{35}S-cysteine cross-labeling of microsomal membrane components was noted within all translation reactions when microsomes were added (Fig. 2B and D). ^{35}S-cysteine cross-labeling increased with longer incubation times, resulted in a higher overall background, and was most evident at 25 kDa (Fig. 2B and D). Isotopically labeled nsp2 translation products were shown to be predominantly full-length nsp2 of an approximate molecular mass of 130 kDa (Fig. 2A), consistent with the expected product size of 129.4 kDa. Additional secondary translation products of lower molecular weight were also faintly visible under normal exposure conditions (1 h exposure; Fig. 2A, black arrows) and could be easily visualized when over-exposed (6 h exposure; Fig. 2C). The expression of either untagged (pNsp2), N-FLAG- (pNsp2 N-FLAG), or C-FLAG-tagged (pNsp2 C-FLAG) nsp2 constructs resulted in the generation of full-length nsp2 protein products of comparable molecular weight (Fig. 2A), however, there were noted differences in the banding pattern of some of the lower molecular weight translation products of pNsp2 N-FLAG (Fig. 2C, lanes 4 and 5). Multiple products between 50 and 75 kDa of the N-FLAG construct displayed a minor upward band-shift as compared to the C-FLAG or the untagged nsp2 expression construct (Fig. 2A and C; black arrows). The lower molecular weight products of the C-FLAG and untagged nsp2 expression constructs displayed similar migration patterns. Temporal studies showed that the lower molecular weight products (> 100 kDa) emerged as early as 15 min during the translation reaction and at times preceded the detectable generation of full-length product (data not shown). Additionally, the appearance of a minor secondary product that migrated at a larger molecular mass (~ 149 kDa) than the complete nsp2 product was also noted. This large 150 kDa protein was an observed product for all nsp2 expression constructs from both closed (circular) (Figs. 2–6) and linearized templates (data not shown). It is important to note that a comparable band with a similar migration pattern was also detected within purified virions by multiple anti-nsp2 antibodies (in contrast to ^{35}S-cysteine labeling) (Kappes et al., 2013). While the composition of this large molecular weight product is unknown, appearance of this band was more evident within the cell-free translation system when nsp2 was expressed in the presence of membranes (microsomes) (Fig. 2B). Addition of microsomes to translation reactions confounded the visualization of the lower molecular weight products, partly due to the noted ^{35}S cross-labeling of microsomal components (Fig. 2B and D, lanes 1 and 2).

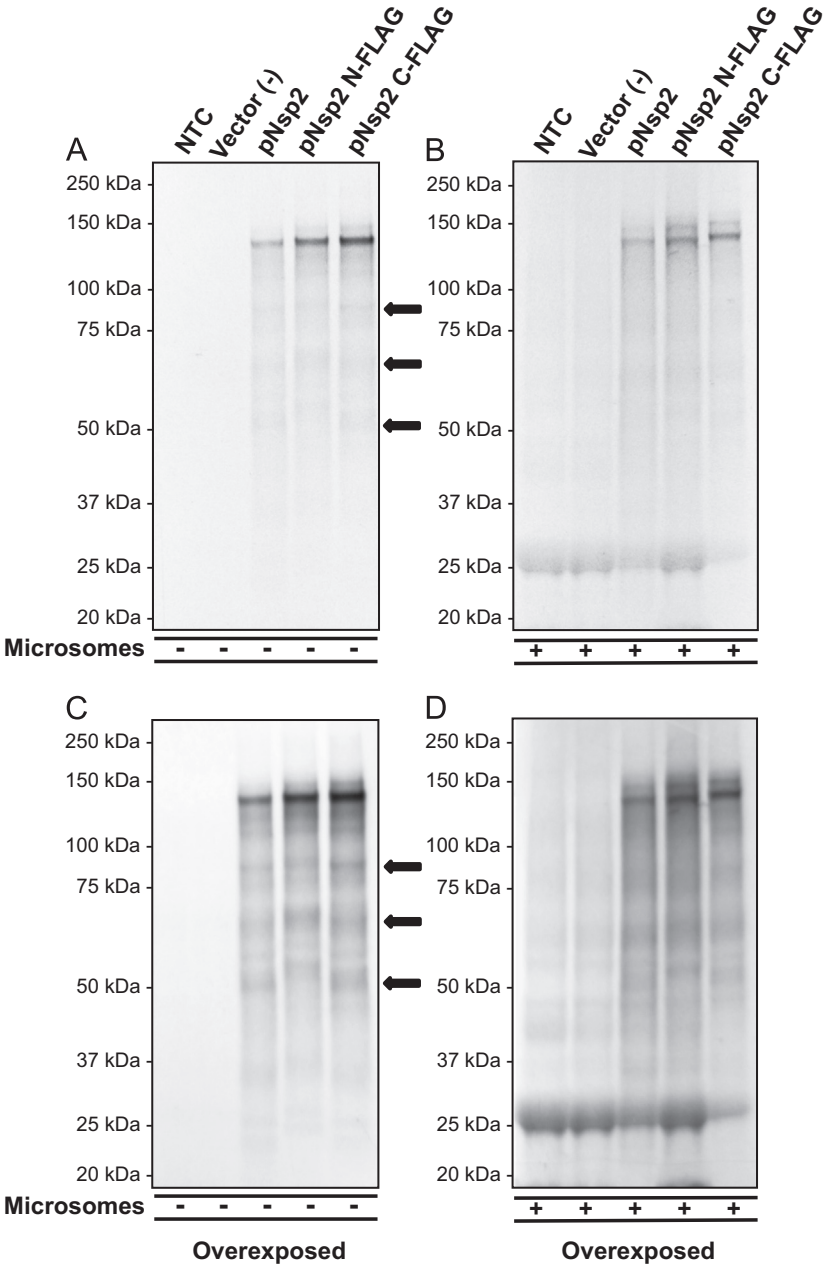

Fig. 2. Cell-free translation of PRRSV nsp2. VR-2332 nsp2 coding region was isotopically labeled by transcription/translation coupled reaction in rabbit reticulocyte lysate with $^{[35]}$S-cysteine either without (A and C) or with (B and D) microsomal membranes. $^{[35]}$S-labeled translation products were loaded at 100,000 counts/lane and PAGE separated under denaturing, reducing conditions in MES running buffer. C) Overexposed image of (A) to highlight the low molecular weight products; (D) overexposed image of (B) to highlight microsomal cross-labeling and low molecular weight products. Lane 1 = Non-template control (NTC), Lane 2 = pcDNA vector control, Lane 3 = pVR-nsp2, Lane 4 = pVR-nsp2 N-FLAG, Lane 5 = pVR-nsp2 C-FLAG.

Nsp2 isoforms differ in PAGE gel banding pattern

Nsp2 translation products were assessed by α-FLAG immunoprecipitation (IP) to define the generation of N-terminal and C-terminal nsp2 isoforms in relation to the full-length product (Fig. 3). As expected, untagged nsp2 expression products were not immunoprecipitated (IP) (Fig. 3A and B; lane 3). IP of FLAG-tagged nsp2 constructs clearly demonstrated differences in generation of N-terminal and C-terminal translation products in the absence of microsomes (Fig. 3A). Numerous N-terminal FLAG-tagged nsp2 products efficiently precipitated at a range between 150 kDa and 5 kDa (Fig. 3 lane 4). In contrast, only two lower molecular weight C-terminal nsp2 isoforms were efficiently precipitated by α-FLAG IP in the absence of membranes (Fig. 3A lane 5). In addition to the full-length nsp2 and the 150 kDa nsp2 protein product, C-terminal isoforms of approximately 73 and 68 kDa were observed (Fig. 3A lane 5). The appearance of secondary products was significantly reduced when nsp2 constructs were expressed in the presence of microsomal membranes (Fig. 3B). A number of molecular products were still observed within the N-FLAG + microsomes IP (Fig. 3B, Lane 4) but were of lower intensity. C-terminal isoforms (C-FLAG + microsomes) comprised only a small fraction of translation reaction products and were only visualized under extreme overexposure conditions, but were able to be visualized (data not shown). IP reactions of nsp2 translation products demonstrate differential banding patterns of N-terminal and C-terminal low-molecular weight translation products (Fig. 3A). Further, the addition of membranes was shown to stabilize the translation reaction yielding predominantly full-length nsp2.

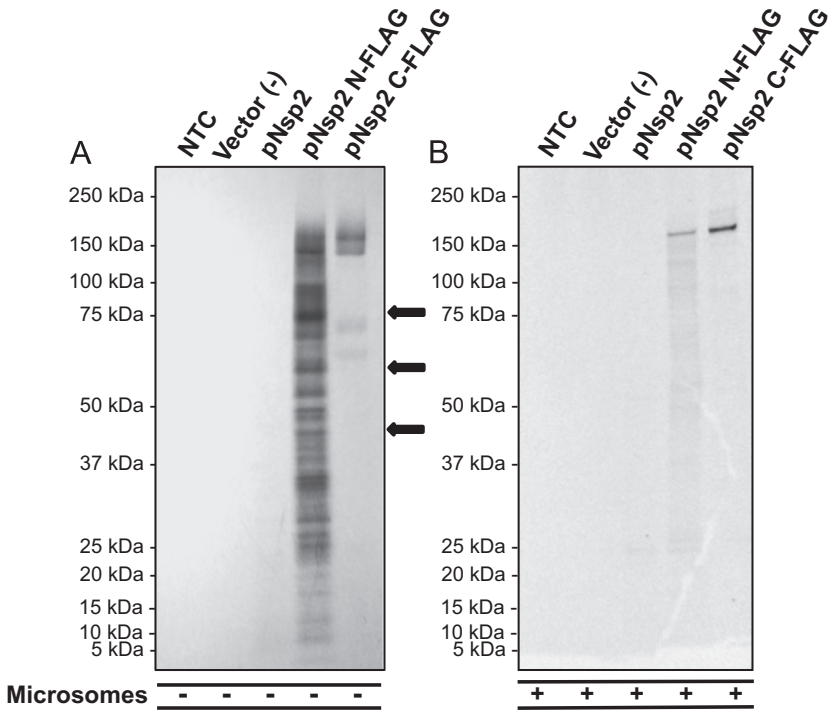

Fig. 3. N-terminal and C-terminal nsp2 isoforms. Translation products generated from reticulocyte lysate expression of nsp2 constructs were immunoprecipitated targeting the FLAG epitope. IP products were PAGE separated under reducing/denaturing conditions. Expression was completed either without (A) or with (B) microsomal membranes. Lane 1=Non-template control (NTC), Lane 2=pcDNA vector control, Lane 3=pVR-nsp2, Lane 4=pVR-nsp2 N-FLAG, Lane 5=pVR-nsp2 C-FLAG.

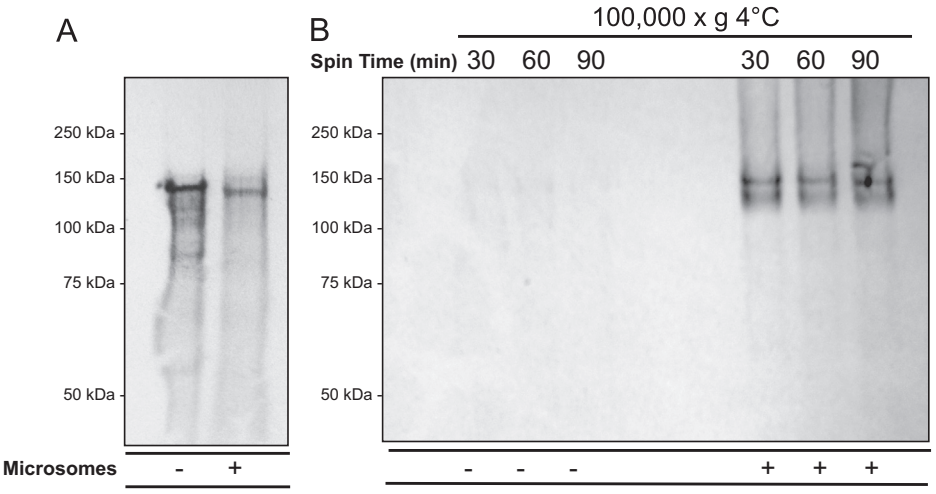

Fig. 4. Nsp2 associates strongly with membranes. [35]S-labeled pNsp2 translation products were expressed either with (+) or without (−) the addition of microsomal membranes. (A) Translation products at 100,000 counts per lane. (B) Translation products equal to 100,000 counts/reaction were pelleted to enrich for the microsomal fraction. Eluted pellets were assessed by PAGE separation under reducing, denaturing conditions.

Nsp2 and select isoforms strongly associate with membranes

Biophysical attributes of some proteins potentiate the association (*i.e.* amphipathic helices) or integration (*i.e.* hydrophobic structures) with membranes. Membrane association of untagged nsp2 (pNsp2) was assessed by isolating the membrane fraction of translation reactions (± microsomes) by high-speed centrifugation. Prior to isolating the membrane fraction, translation reactions of both nsp2 (− microsomes) and nsp2 (+ microsomes) were first assessed by PAGE (Fig. 4A). As noted previously, multiple subdominant low molecular weight bands were observed products of each translation reactions (Fig. 4A). To determine the relative pelleting efficiencies of ^{35}S-cysteine labeled nsp2, either without microsomes (Fig. 4B; − microsomes) or with microsomes (Fig. 4B; +microsomes), equal counts of each translation reaction was pelleted by high-speed ultracentrifugation in isotonic buffer to isolate the membrane fraction, as outlined in the materials and methods. As expected, in the absence of microsomes, ^{35}S-cysteine labeled nsp2 was not detected, demonstrating free nsp2 is not isolated within the membrane fraction (Fig. 4B; − microsomes). Extending centrifugation time four-fold further failed to isolate detectable free nsp2 (−microsomes). In contrast, nsp2 expressed in the presence of membranes (+ microsomes) was efficiently isolated in the membrane fraction within the first 30 min at 100,000g (Fig. 4B; +microsomes). Increasing spin times four-fold did not increase isolation of membrane bound product (Fig. 4B; + microsomes). The results demonstrate the strong association of full-length nsp2 with membranes.

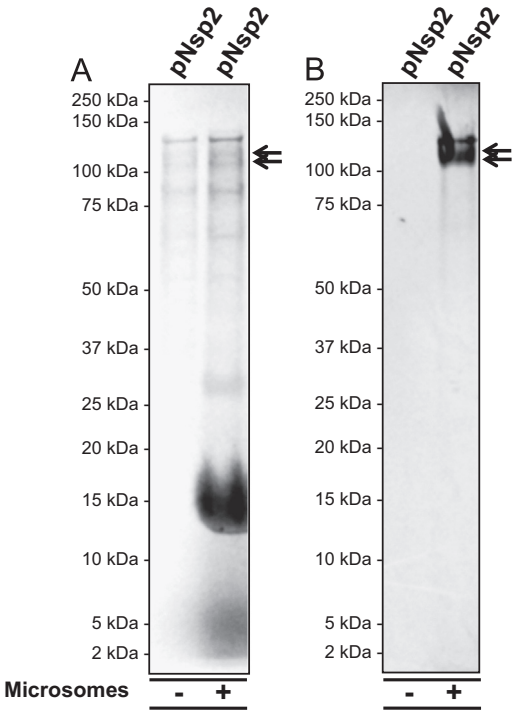

Fig. 5. Membrane enrichment of select nsp2 isoforms. pVR-nsp2 $^{[35]}$S-labeled translation products were expressed either with or without canine microsomal membranes. Lane 1=(−) microsomes, Lane 2=(+) microsomes. (A) Translation reactions PAGE separated under reducing, denaturing conditions. (B) Translation products equal to 100,000 counts/reaction were pelleted at 150,000*g* for 1 h to enrich for the microsomal fraction. Eluted pellets were assessed by PAGE separation under reducing, denaturing conditions. Black arrows indicate the approximate molecular weight of enriched nsp2 sub-dominant products.

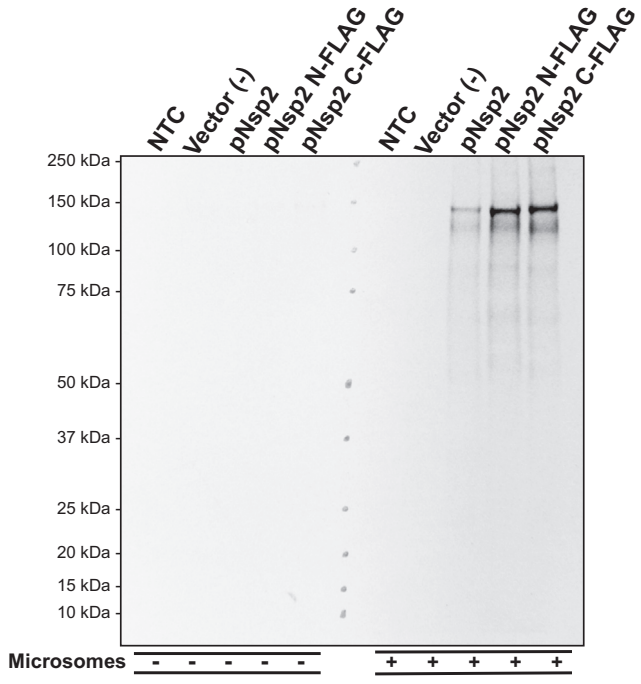

Fig. 6. Membrane enrichment of FLAG-tagged products. $^{[35]}$S-labeled translation products were expressed either with or without canine microsomal membranes. Products were pelleted at 150,000*g* (4 °C) 1 h. Eluted pellets were subjected to PAGE separation under reducing, denaturing conditions. Lane 1=Non-template control (NTC), Lane 2=pcDNA vector control, Lane 3=pVR-nsp2, Lane 4=pVR-nsp2 N-FLAG, Lane 5=pVR-nsp2 C-FLAG.

Surprisingly, a second lower molecular weight product between 120 and 100 kDa was also found to be strongly membrane associated (Fig. 4;+microsomes). This secondary product was observed to not only be membrane associated but appeared to be enriched within the membrane fraction. The nsp2 translation product(s) migrating between ~120 and 100 kDa was consistently observed to be a sub-dominant translation product within the original translation reaction (Figs. 2A and 4A,+microsomes) but appeared of equal intensity to the full-length (dominant) product within the membrane fraction (Fig. 4B,+microsomes). A repeat of this experiment allowed a more detailed resolution of these nsp2 expression products (± microsomes; Fig. 5A). The dominant product at or around 15 kDa within the unpurified cell-free translation (+ microsomes only) is due to microsomal cross-labeling by ^{35}S, similar to the observed cross-label observed in Fig. 2B and D. The 120−100 kDa band was found to be two distinct products of approximately 117 and 106 kDa (Fig. 5A, black arrows). Isolation of the membrane fraction again showed the efficient isolation of these membrane associated nsp2 products only (+ microsomes; Fig. 5B). In addition to the full-length nsp2 product, the lower molecular weight nsp2 isoforms of approximately 117 and 106 kDa (Fig. 5A, black arrows) co-purified in the membrane fraction (Fig. 5B, black arrows). All other low molecular weight translation products (>100 kDa) originally noted within the native translation reaction were not isolated within membrane fraction; demonstrating enrichment of a fraction of the nsp2 translation products (Fig. 5A and B). These membrane isolation studies show the selective incorporation of nsp2 translation products, including the full-length nsp2 and two large nsp2 isoforms, within the membrane fraction.

Nsp2 is an integral membrane protein

To assess whether the introduction of the FLAG-tag epitope to either the N- or C-terminus of nsp2 altered the ability of nsp2 to associate with membranes, the membrane fraction of N-FLAG and C-FLAG nsp2 expression products were assessed in relation to the untagged nsp2 (pNsp2) (Fig. 6). As noted previously, the expression of the pCDNA vector only, or the NTC, did not result in the generation of any detectable protein product (Fig. 6, lanes 1 and 2; left and right panels respectively). As expected, when microsomes were not added to the translation reaction, no products were isolated within the membrane fraction (Fig. 6; − microsomes lanes 4−5). Expression of N-FLAG and C-FLAG nsp2 constructs in the presence of microsomal membranes resulted in the efficient isolation of nsp2 within the microsomal fraction, similar to that of the untagged nsp2 (Fig. 6;+microsomes). These results show that the FLAG epitope on either the N- or C-terminal coding regions of nsp2 does not affect membrane association of nsp2.

To test whether nsp2 functions as an integral membrane protein, the isolated membrane fraction of each translation product was subjected to proteinase K digestion [protease protection assays (PPA)]. Protein domains that have either embedded within the membrane or that have traversed the bilayer and are enclosed within the luminal surface of the microsomes will be protected from protease digestion (Faaberg and Plagemann, 1995). Proteinase K PPA products were assessed by PAGE to define ^{35}S-cysteine labeled product protected from digestion (Fig. 7). As expected, in the absence of membranes, translation reactions were fully digested and no detectable fragments remained. In the presence of membranes (+ microsomes), PPA from each nsp2 expression construct, but not from the NTC or the pcDNA vector control, produced a single protected fragment of 13–15 kDa in size (Fig. 7). The protected fragment of N-FLAG, C-FLAG, and untagged nsp2 constructs appeared identical in migration and intensity indicating similar membrane association efficiency and retention (Fig. 7, lanes 3–5). These results together demonstrate nsp2 integrates within microsomal membranes and that a product of approximately 15 kDa is protected from digestion

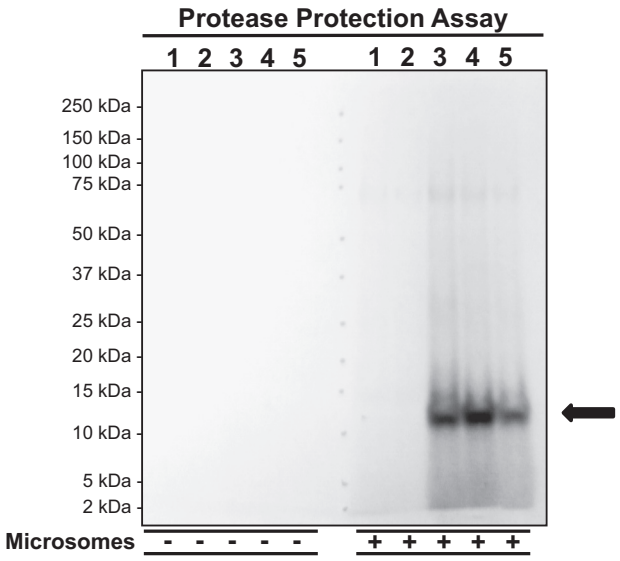

Fig. 7. Nsp2 fragment is protected from protease degradation by membrane insertion. [35]S-labeled translation products were expressed either with or without canine microsomal membranes. Products were pelleted at 150,000*g* (4 °C) 1 h. Membrane associated nsp2 was subjected to protease protection assay (proteinase K digestion) as outlined in the materials and methods and assessed by PAGE separation under reducing, denaturing conditions. Lane 1=Non-template control (NTC), Lane 2=pcDNA vector control, Lane 3=pVR-nsp2, Lane 4=pVR-nsp2 N-FLAG, Lane 5=pVR-nsp2 C-FLAG.

either through integration within the membrane bilayer (transmembrane helices) or through orientation within the luminal surface of the microsomal compartment.

Nsp2 membrane integration yields an unexpected topology

PPA experiments demonstrated a ~15 kDa fragment was protected from proteinase K digestion, defining nsp2 insertion into microsomal membranes. Two distinct domains of nsp2 are noted to be similar in size to the observed PPA fragment, the putative multi-pass transmembrane domain (TM1-5; 17 kDa) and the downstream C-terminal domain (20 kDa). To further define the topology of nsp2, and to identify the protected domain of nsp2, PPA products were subjected to IP analysis (Fig. 8A). IP analysis of PPA protected fragments clearly demonstrated the 15 kDa fragment originated from the C-terminal domain (Fig. 8A). The protected fragment from the PPA of the untagged nsp2 construct did not precipitate by IP pull-down, demonstrating the IP reaction specifically targets FLAG-tagged products from the PPA reaction (Fig. 8A; lane 3). While the N-FLAG tagged nsp2 PPA product failed to precipitate by α-FLAG IP (Fig. 8, lane 4), two C-terminal FLAG tagged nsp2 products of approximately 15 kDa and 5 kDa were identified in the IP pull-down of PPA reactions. It is unknown if the 5 kDa protein was enriched within the IP reaction or if it is a partially digested product. Partially digested products could result from low amounts of incompletely inactivated proteinase K incubated for long time points ($\geq$18 h) during the IP reaction. These results clearly demonstrate the C-terminal domain of nsp2 adopts a transmembrane or luminal topology. Further, the large hydrophilic N-terminal domain (PLP2 and HV; ~90 kDa) was not observed to be protected from digestion, indicating a cytoplasmic orientation. These results define an unexpected topology of nsp2 where the large N-terminal domain is maintained on the cytoplasmic surface and the C-proximal hydrophobic region integrates within the membrane orientating the C-terminal domain within the luminal surface.

Discussion and conclusion

Fig. 1A proposes a simple diagram of PRRSV replicase integral membrane proteins as outlined by the predicted hydrophobicity strength scores (TMHMM) of the entire ORF1a polyprotein. The transmembrane prediction of the ORF1a hydrophobic domains (Fig. 1A; green line) depicts multiple regions where the number of TM helices are inconclusive. Of the three putative ORF1a transmembrane proteins, nsp2 transmembrane prediction is the most unclear. Utilizing nine separate bioinformatic algorithms further showed variation with respect to both the predicted transmembrane helices (location) as well as the number of transmembrane spanning domains (Table 1). The ultimate number of functional transmembrane domains encoded and the resulting topological orientation (in/out) (Fig. 1B, 1–4) has important implications on the mechanism of ORF1a/b polyprotein processing, orientation of downstream ORF1a putative transmembrane proteins, and on potential function(s) of nsp2 within the viral reticulovasicular network (RVN) (Knoops et al., 2012). Because of these unknowns we sought to define the functionality of the putative transmembrane domains and further define the topological orientation of nsp2.

Since strong viral protein–protein interactions can complicate assessment of native transmembrane insertion (van der Meer et al., 1998), and additionally PRRSV nsp2 interacts with a wide range of cellular proteins (Wang et al., 2014), we chose to complete these initial studies on nsp2 transmembrane functionality within a reductionist cell-free translation system in the absence of all other viral proteins.

In this report the membrane association of both nsp2 and select isoforms was demonstrated and the integral nature of nsp2 was defined. Expression of nsp2 within reticulocyte lysate resulted in multiple sub-dominant protein products in addition to the full-length nsp2, similar to the banding pattern previously described (Kappes et al., 2013), including a faint triplicate between 80 kDa and 60 kDa and a tight duplet/triplicate at or near the 50 kDa range (Fig. 2). IP pull-down of the C-terminal FLAG-tagged nsp2 construct further identified lower molecular weight products as isoforms of nsp2 (Fig. 3). It is currently unclear how these low molecular weight isoforms are generated but have been proposed to be through differential cleavage of the full-length nsp2 (Han et al., 2010).

Definitive differences in banding patterns between N-terminal (N-FLAG) and C-terminal (C-FLAG) were observed from IP reactions (Fig. 3). The abundance of lower molecular weight bands within the N-FLAG IP reactions are suspected to be, at least in part, abortive translation products (Han et al., 2010). Translation within the cell-free system (reticulocyte) of a large 130 kDa (1196aa) protein is near the upper range for this assay and could help explain many of the minor secondary N-terminal translational products (N-FLAG). Abortive translation products however would not explain the clearly defined low molecular weight C-terminal nsp2 isoforms observed within α-FLAG IP reactions (C-FLAG). It is probable that the defined bands between 50 kDa and 75 kDa (Fig. 3) were generated through cleavage of the nsp2 protein by an as yet undefined mechanism. Initial attempts were made to express nsp2 within the reticulocyte system in the presence of multiple protease inhibitors, all of which completely aborted translation (data not shown). Addition of microsomes to the translation reaction clearly stabilized nsp2 expression, potentiating generation of predominantly full-length nsp2 product (Fig. 3B). Isolation of the membrane (microsomal) fraction demonstrated the strong association of not only the full-length nsp2 protein (Fig. 4) but additionally the enrichment of two nsp2 isoforms migrating at approximately 117 kDa and 106 kDa (Fig. 5). These results remained consistent with the isolation of membrane bound FLAG-tagged nsp2 constructs (Fig. 6). The isolation of two tightly membrane associated nsp2 isoforms was surprising since enrichment in banding intensity (from sub-dominant translation products to dominant products within the membrane fraction) suggest a

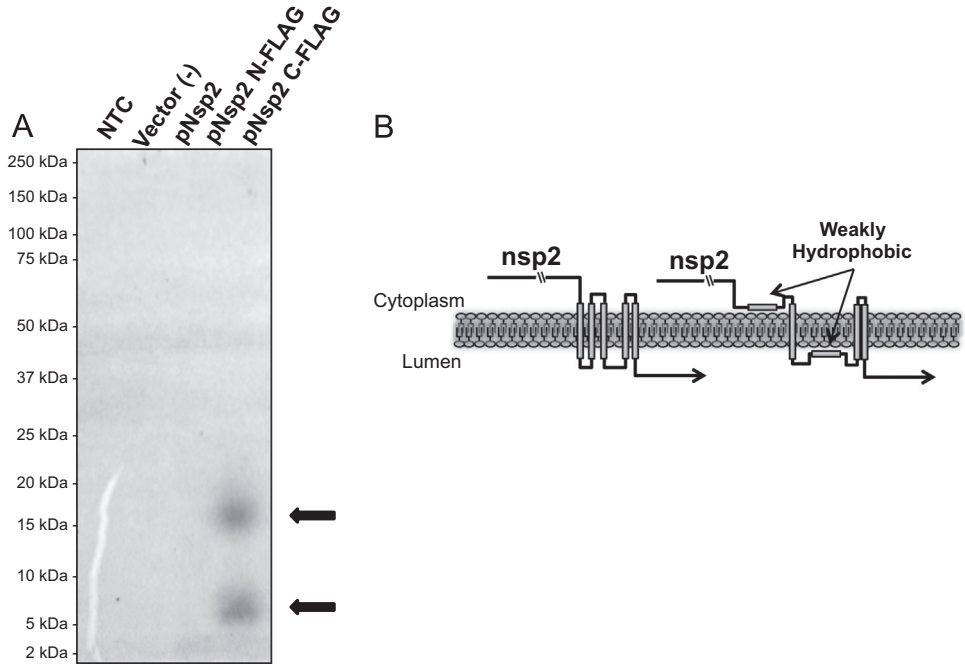

Fig. 8. The C-terminus of nsp2 is protected from protease degradation by membranes. (A) Translation products were expressed in the presence of microsomes. [35]S-labeled translation products were stabilized in TBSS and an enriched microsomal fraction was generated through pelleting at 150,000*g* 1 h. The pelleted fraction was digested with proteinase K (protease protection assay) and further processed by immunoprecipitation, targeting the exogenous FLAG epitope (α-FLAG). Lane 1=Non-template control (NTC), Lane 2=pcDNA vector control, Lane 3=pVR-nsp2, Lane 4=pVR-nsp2 N-FLAG, Lane 5=pVR-nsp2 C-FLAG. B) Graphical representation of the predicted membrane associated functions of the weakly hydrophobic putative transmembrane domains TM1 and TM3.

Table 1
Prediction of nsp2 transmembrane helices. Nsp2 (VR-2332 (DQ217415)) transmembrane domains, numbered corresponding to nsp2 amino acid position, were assessed by bioinformatic predictive algorithms Phobius (Kall et al., 2004); HMMTOP 2.0 (Tusnady and Simon, 2001); SCAMPI (Bernsel et al., 2008); TOPCONS (Bernsel et al., 2009); OCTOPUS (Viklund and Elofsson, 2008); PRO/PRODIV-TMHMM (Viklund and Elofsson, 2004); and MemBrain [TMH prediction; (Shen and Chou, 2008)] using default settings unless otherwise noted in the materials and methods. On average, most prediction algorithms define four transmembrane spanning domains (TM1−4); however, the aggregated output from the nine predictive programs defines a total of five transmembrane spanning helices (Regions 1–5).

	TM1		TM2		TM3		TM4		TM5
Phobis	845-865		877-903		910-926		960-979		988-1006
HMMTOP	849-866		879-903		912-936		963-981		988-1006
SCAMPI-seq		874-894		907-927		960-980		986-1006	
SCAMPI-msa		874-894		906-926		960-980		988-1008	
PRODIV	844-864		877-904		907-927			988-1008	
PRO		875-895		906-926		962-982		987-1007	
OCTOPUS		874-894		906-926		960-980		988-1008	
TOPCONS		874-894		906-926		960-980		988-1008	
MemBrain	852-863		874-902		911-927			983-1007	
	Region 1		Region 2		Region 3		Region 4		Region 5

tighter interaction with the membrane compared to the full-length product. Further, these isoforms are consistent in size to the previously reported translational isoforms nsp2TF and nsp2N generated through −2 RFS and −1 RFS, respectively (Fang et al., 2012b). While the critical requirement of nsp1β for efficient RFS within transmembrane region 1 (TM1) of nsp2 was recently demonstrated (Li et al., 2014), strongly suggesting these are not translational isoforms, it is important to note that the −2 RFS dramatically changes the predicted hydrophobicity of the multi-spanning transmembrane region strongly favoring membrane insertion (Fig. 9). Initial deglycosylation studies of microsomal associated nsp2 products found no evidence of glycosylation of full-length nsp2 or nsp2 isoforms within the cell-free translation system, however further assessment is needed within in vitro and *ex vivo* systems.

Nsp2 membrane integration was conclusively determined and the topology defined through investigations utilizing protease protection assays (PPA) against proteinase K digestion (Fig. 7). Results demonstrated a small fragment was protected from digestion, defining membrane insertion, and IP further confirmed the protected fragment (15 kDa) was derived from the C-terminus (Fig. 8A). The integration of nsp2 with a topological orientation yielding N- and C-termini on opposing sides of the membrane is counterintuitive

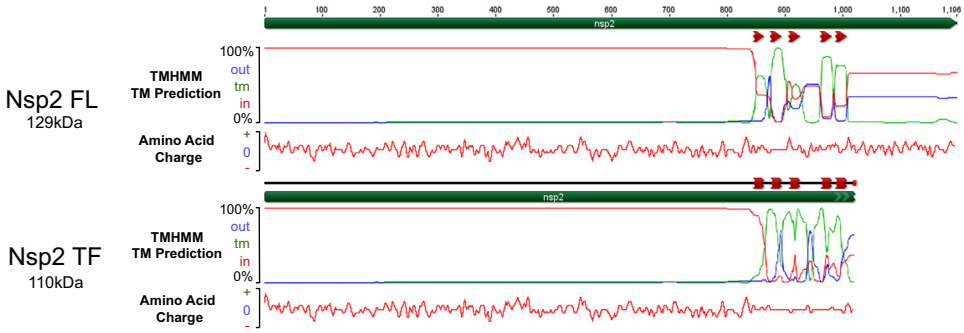

Fig. 9. RFS alters the hydrophobicity profile of nsp2. Predicted hydrophobicity profiles using the TMHMM algorithm depicted for both the full-length nsp2 (VR-2332) and nsp2-TF (-2 RFS). Red arrows denote the putative transmembrane helices as defined by the TOPCONS prediction algorithm. Green lines define the predicted probability of an encoded transmembrane domain (TMHMM) from 0% (bottom) to 100% (top). Images were generated using the Geneious software platform.

since the established polyprotein processing cascade requires the PLP2 (OTU) protease domain and the nsp2–3 junction site be contiguous and not impeded by physical barriers. However, the historical rules of membrane integration and 'positive-inside' topology (von Heijne and Gavel, 1988) has been muddled by recent unexpected findings from the growing number of solved high-resolution structures of integral membrane proteins and correlative biological data (von Heijne, 2011). Observed topological variations include dual-topology proteins ("flip-flopping" or "indecisive" integration) (Rapp et al., 2006), mixed or diverse topological profiles of monotopic (Ott and Lingappa, 2004) and polytopic membrane proteins (Skach et al., 1993; Zhang and Ling, 1991) (topological heterogeneity), and temporally dynamic topologies which either re-orient post-translationally (Lu et al., 2000) or, as in the case of the hepatitis B large envelope glycoprotein (L), a fraction (~50%) re-orients in a protracted Hsc70/Bip chaperone-mediated process (Lambert and Prange, 2003) (dynamic topologies). Topological variation has, at least in part, been attributed to inefficiencies in integration of weakly hydrophobic domains (Ota et al., 1998; von Heijne, 2006). As noted in Fig. 1, nsp2 encodes three regions of strong hydrophobicity (VR-2332 nsp2 874–902aa, 960–980aa, and 986–1007aa) and two weaker hydrophobic domains (nsp2 845–864aa and 906–927aa) (Fig. 1). Further assessment of the nsp2 hydrophobic region by the use of multiple bioinformatic predictive programs showed that while most algorithms define a succinct set of four potential transmembrane domains (Table 1; TM1–4), the aggregated output of the nine separate bioinformatic transmembrane/hydrophobicity predictive algorithms describe a total of five distinct putative transmembrane helices within PRRSV nsp2 (Table 1; Regions 1–5).

Originally, we postulated that one of the two weak hydrophobic domains would not be functional (Fig. 1B, 1 and 2) in order to maintain an even number of transmembrane domains, allowing for the *cis*-cleavage of the nsp2↓nsp3 junction following co-translational integration within the membrane. However, alternative pathways allowing for membrane integration and proteolytic processing are possible based on existing data. The physical separation of the large cytoplasmic PLP2 protease domain and the luminal C-termini by the membrane interface would require that polyprotein processing of the nsp2↓nsp3 junction to be cleaved either in *trans* following membrane insertion, or that cleavage of nsp2↓nsp3 precedes membrane insertion. Similarly, current data supports both as possibilities; that the PLP2 exhibits both *cis*- and *trans*- cleavage activities (Han et al., 2009) and that nsp2 has been also shown to interact with cellular chaperones known to participate in post-translational membrane integration (Wang et al., 2014). Most simply, any nsp2 isoform resulting from a cleavage event between the PLP2 protease domain and the TM region would allow for physical separation of these domains and thus differential localization. While this would allow for unbound nsp2 N-terminal (PLP2) isoforms to migrate to the nsp2–3 junction and process this site in *trans*, detailed studies defining the genesis of these cleavage isoforms are needed. Additionally, an N-terminal ER targeting sequence has not been identified, making it unlikely these unbound isoforms (most between 50 and 120 kDa; Fig. 3) would be able to traverse to the luminal side of the ER to access the nsp2↓nsp3 junction at early time points during infection (prior to DMV/RVN formation). At later time points after DMV formation, nsp2 localizes diffusely within the perinuclear region (Kappes et al., 2013; Li et al., 2012) and thus it is possible that *trans*-cleavage specificity could play some role at this stage.

Alternatively, post-translational insertion of proteins into the ER membrane has been shown to occur via multiple pathways including signal recognition particle (SRP)-dependent (Abell et al., 2004), heat-shock protein 70 (HSP70)-dependent (Abell et al., 2007), and 'unassisted' (Brambillasca et al., 2006, 2005) mechanisms. As a nascent apolar peptide emerges from the ribosomal tunnel, it requires immediate shielding from the aqueous cytosolic environment to protect against inappropriate folding or aggregation, either through direct membrane insertion (co-translational insertion) (Nagai et al., 2003) or chaperone mediated nascent protein shielding (post-translational integration pathways) (Abell et al., 2007; Leznicki et al., 2010). PRRSV nsp2 has been found to interact with multiple cellular proteins associated with translational regulation and membrane insertion, particularly the chaperone protein human leukocyte antigen (HLA)-B-associated transcript 3 (Bat3/Bag6/Scythe) (Wang et al., 2014). Bat3 is a multi-functional chaperone protein that plays a central role in regulation of post-translational ER membrane targeting (Leznicki et al., 2010, 2013; Mariappan et al., 2010), ubiquitin-dependent ER-associated protein degradation (ERAD) proteome targeting (Wang et al., 2011), and removal and degradation of mislocalized proteins (Hessa et al., 2011). Bat3 functions by binding to nascent hydrophobic polypeptides as they emerge from the ribosomal tunnel, specifically binding long stretches of hydrophobic residues (Lee and Ye, 2013; Mariappan et al., 2010), maintaining hydrophobic proteins in a soluble state until membrane insertion (Leznicki et al., 2010). In addition, nsp2 has been found to also interact with other ER chaperone proteins implicated in post-translational membrane integration, HSP70 (Abell et al., 2007; Wang et al., 2014) and binding immunoglobulin protein (Bip/GRP78/HSPA5) (Han et al., 2010; Rapoport, 2007). Bat3 appears to play a fundamental role in association with both of these proteins whereas Bat3 promotes the stability of HSP70 and Bip (Corduan et al., 2009; Sasaki et al., 2008). Bat3 and related holdase machinery (TRC35/UBL4) are present within reticulocyte lysates (Mariappan et al., 2010).

Whether a transmembrane protein is processed co-translationally or post-translationally, and which mechanism/pathway is utilized, most often relies on attributes of protein coding sequence adjacent to or within the hydrophobic area (Abell et al., 2003, 2004; Kang et al., 2006; Ott and Lingappa, 2004; van Geest and Lolkema, 2000; von Heijne, 1985; Walter and Johnson, 1994). However, the 'rules' dictating how protein sequence imparts these regulatory signals are currently not well understood (Seppala et al., 2010). It is important to

Table 2
Sequence of oligonucleotides for insertion of exogenous FLAG epitope. Bold = nsp2 coding sequence; parenthesis restriction enzyme site; underlined = FLAG Epitope.

Name	Primer sequence
5′FLAG SDM Forward	5′-TTAATTAAGCCGCCGCCATG(CCTGCA↓GG)**GCTGGAAAGAGAGCAAGAAA**
5′FLAG SDM Reverse	5′-**TTTCTTGCTCTCTTTCCAGC**(CC↑TGCAGG)CATGGCGGCGGCTTAATTAA
3′FLAG SDM Forward	5′-**TTTCCAAGCCTTCAGGGGGA**(CCTGCA↓GG)ATCACTAGTGAATTCGCGGC
3′FLAG SDM Reverse	5′-GCCGCGAATTCACTAGTGAT(CC↑TGCAGG)**TCCCCCTGAAGGCTTGGAAA**
FLAG Forward	5′-ATTATT(CCTGCA↓GG)CGACTACAAAGACGATGACGACAAGA(CCTGCA↓GG)CGCAGCA
FLAG Reverse	5′-TGCTGCG(CC↑TGCAGG)TCTTGTCGTCATCGTCTTTGTAGTCG(CC↑TGCAGG)AATAAT

mention that all chaperone proteins that interact with nsp2 also participate in a diverse set of functions, and that interaction with nsp2 does not necessitate it is exclusively for post-translational roles associated with membrane integration. However, a core function of Bat3 is to bind hydrophobic regions of proteins in order to maintain solubility while a triage (protein quality control) decision is made regarding ER targeting or ubiquitin-dependent destruction (Lee and Ye, 2013). While it is postulated that Bat3 would function to directly target nsp2 for post-translational membrane insertion, the PLP2 protease possesses deubiquitinating functionality (Deaton et al., 2014; Frias-Staheli et al., 2007) that, if targeted for destruction, may rescue nsp2 from ULB4 ubiquitin-dependent degradation and further potentiate ER membrane targeting.

In this report we demonstrated that nsp2 is an integral membrane protein that possesses a cytoplasmic/luminal topological orientation within the context of the cell-free in vitro translation assay. Research has shown that retention of proteins in membranes does not exist as a static state and the environment of the polar/apolar surface is dynamic and is managed by a range of physical forces and biological intermediaries (Ota et al., 1998; Seppala et al., 2010; von Heijne, 1985; von Heijne and Gavel, 1988; White and von Heijne, 2008). Future research is needed to define the membrane integration steps of nsp2, whether co-translationally or post-translationally, and what the cellular and viral interacting partners may be. Stepping up studies into cellular in vitro and *ex vivo* systems using vectored nsp2, ORF1a, or competent infection studies should show if interaction with additional cellular or viral components induce altered integration or varied topologies. As noted earlier, nsp2 encodes two weak hydrophobic elements of unknown functionality (Fig. 8B). Initial attempts to map the transmembrane coding helices through mutational analysis failed to conclusively define which elements associate or embed within the membrane and require further investigation (data not shown). Studies showed a strong association of the full-length nsp2 and two large nsp2 isoforms with membranes (Fig. 5); and further demonstrated that the C-terminus of nsp2 is translocated to the lumen surface of canine pancreatic membranes (Figs. 7 and 8). These results define nsp2 as an integral membrane protein of PRRSV. The demonstrated membrane integration of nsp2 within this report supports previous predicted functions of nsp2 associated with membrane rearrangement and association with the PRRSV virion. Identification of a small class of membrane associated nsp2 isoforms of unknown function further highlight the complex composition of nsp2.

Materials and methods

Construction of expression plasmids

pVR-2332 (DQ217415) template was amplified (Platinum Taq, Invitrogen) using custom DNA primers VR-nsp2-F: 5′-*GCT GGA AAG AGA GCA AGA AAA GCA CG*-3′ (VR-2332 nt 1325–1350) and VR-nsp2-R: 5′-*TCC CCC TGA AGG CTT GGA AAT TTG C*-3′ (VR-2332 nt 4888–4912) targeting the complete nsp2 coding region (VR-2332 nt 1325–4912). Amplified products were gel purified using the QIAquick gel extraction kit [Qiagen] and underwent a second round of amplification (Phusion® High-Fidelity DNA polymerase, NEB) and gel purification. Purified PCR products were incubated with 12 mM dATP [New England Biolabs (NEB)], GoTaq Flexi DNA polymerase (1.25 U), and GoTaq reaction buffer (1 × ; 1.5 mM $MgCl_2$) [Promega] at 72 °C for 20 min to introduce 3′ A-tail overhangs. A-tailed products were purified to remove reaction components [Zymogen Clean and Concentrator-5] and A – T cloned into the pGEM®-T EASY vector system per manufacturer's instructions (Promega). Resulting ligations were transformed into either JM-109 (Promega) or Mach1 (Invitrogen) chemically competent cells per manufacturer's instructions. Positive ligation clones grown under ampicillin resistance (100 ug/ml; Sigma) were amplified and screened by restriction digest and sequenced for positive 5′-end to 3′-end directional insertion. Correct clones were sequenced to cover the entire nsp2 coding region and flanking vector sequence. Two point mutations that altered the amino acid coding sequence were identified and restored to parental sequence with the QuikChange II XL site-directed mutagenesis kit (Agilent) and custom DNA mutagenesis primers. Additional restriction digestion and site-directed mutagenesis was completed directly upstream of the nsp2 5′ coding sequence to remove inefficient upstream start codons and an upstream NotI restriction site, and to introduce a novel PacI restriction site and a strong Kozak sequence upstream of the start codon (5′-*GCCGCCGCCAUG*-3′). The pcDNA 3.0 cloning vector was also altered by site-directed mutagenesis to introduce a novel PacI restriction site directly upstream of the NotI restriction site (to facilitate directional cloning) by changing the sequence 5′-CATCACAC-3′ (vector sequence 954 – 961nt) to TTAAT↓TAA. pGEM-Nsp2 clones were digested with PacI and NotI restriction enzymes and the nsp2 insert was selected and gel purified [QIAquick gel extraction kit, Qiagen]. Purified inserts were directionally cloned into the pcDNA 3.0 expression vector downstream of the T7 transcription initiation sequence using the PacI/NotI restriction sites and the Blunt/TA ligase master mix [NEB]. The resulting expression construct was denoted as pNsp2 (1-1196aa).

To facilitate immunoprecipitation assays, expression constructs were engineered to encode an exogenous FLAG epitope (DYKDDDDK) either at the 5′ termini (pNsp2 N-FLAG) or directly downstream of the nsp2 coding region (pNsp2 C-FLAG). Intermediate pNsp2 clones were engineered to possess a SbfI restriction site (CCTGCA↓GG) by site-directed mutagenesis (pNsp2 5′SbfI: [AUG (CCTGCA↓GG) **GCT GGA AAG**… -3′]; pNsp2 3′SbfI: [5′- …**TCA GGG GGA** (CCTGCA↓GG)…-3′], bold = nsp2 sequence) flanking the 5′ or 3′ termini of nsp2 (Table 2). A pair of synthetic oligonucleotides encoding the FLAG epitope (FLAG Forward and FLAG Reverse) was designed to encode flanking SbfI restriction sites (Table 2). The FLAG oligonucleotides were annealed by first heating to 95 °C and then reducing the temperature 1 °C/min in a thermocycler [Eppendorf] until 20 °C is

reached. The annealed FLAG oligonucleotides were digested by SbfI and ligated into pNsp2 5′SbfI or pNsp2 3′SbfI at a 1:1 M ratio to generate in-frame FLAG-tagged expression constructs pNsp2 N-FLAG and pNsp2 C-FLAG, respectively.

Bioinformatic predictions

pVR-2332 (DQ217415) nsp2 protein coding sequence was analyzed by the transmembrane prediction algorithms Phobius ['Normal prediction' method; (Kall et al., 2004)]; HMMTOP 2.0 (Tusnady and Simon, 2001); SCAMPI (Bernsel et al., 2008); TOPCONS (Bernsel et al., 2009); OCTOPUS (Viklund and Elofsson, 2008); PRO/PRODIV-TMHMM (Viklund and Elofsson, 2004); and MemBrain [TMH prediction; (Shen and Chou, 2008)] using default settings unless otherwise noted.

Cell-free translation of nsp2

Nsp2 expression constructs were translated using the TNT® T7 coupled transcription/translation reticulocyte lysate system (Promega) with some modifications to the manufacturer's instructions. The rabbit reticulocyte lysate was thawed quickly at 37 °C prior to being placed on ice, all other components including the diluent (H_20) and DNA template were chilled to 4 °C before assembling translation reactions. Reactions were assembled on ice using 1 ug DNA template per 25 μl translation reaction either with or without the addition of canine pancreatic microsomal membranes (microsomes; Promega; see below). RNasin® Plus RNase inhibitor (Promega) was added to each reaction (1.6 U/μl per rxn) to inhibit RNA degradation during the translation reaction. It was important to increase the amino acid mixture [minus cysteine] (Promega) 3-fold to a 0.06 mM final concentration to enable efficient translation of the large 129 kDa nsp2 protein. All other reaction components were added per manufacturer's specifications. $^{[35]}$S-cysteine (Cysteine L-[35S]; 10 μCi/μl; PerkinElmer) thawed on ice was added to the translation reaction after all other components (0.4 mCi/ml final concentration). When used, microsomes were added to the translation reaction as a final step at a dilution of 1 μl microsomes per 25 μl translation reaction volume. The reaction was then mixed gently followed by incubation at 25 °C for 1 h. Lowering the incubation temperature to 25 °C was found to aid expression of full-length nsp2 product. All reactions were then quickly chilled to 4 °C. Translation products were quantified by measuring the amount of incorporated product (scintillation counts; Promega #TB126) prior to use in downstream assays.

Polyacrylamide gel electrophoresis

Reactions to be assessed by polyacrylamide gel electrophoresis (PAGE) were diluted to 15 μl in phosphate-buffered saline (PBS; 10 mM Na_2HPO_4/KH_2PO_4, 137 mM NaCl, pH 7.4) as needed. Samples were reduced with 4 × NuPAGE® LDS sample buffer (Life Technologies) supplemented with 10% v/v DTT (500 mM; Life Technologies) and 30% w/v urea (Mallinckrodt). Reducing buffer was added to a 1 × final concentration followed by heat denaturation at 100 °C for 5 min. Reduced and denatured samples were loaded onto NuPAGE® Novex® 4–12% Bis-Tris polyacrylamide gels (Life Technologies) and electrophoresed at constant voltage in 1 × Novex® 2-(*N*-morpholino)ethanesulfonic acid running buffer (MES; 145 V) (Life Technologies) or 1 × Novex® 3-(N-morpholino)propanesulfonic acid running buffer (MOPS; 125 V) (Life Technologies) supplemented with NuPAGE® antioxidant (Life Technologies) per manufacturer's instructions. PAGE separated gels were incubated in gel drying buffer [50% methanol (HPLC grade; Honeywell), 7.5% glacial acetic acid (Fisher Chemical), and 10% glycerol (ACS grade; Macron)] for 30 min at room temperature (RT), further dehydrated in 200 proof ethanol (ETOH, Decon Laboratories) for 15 min at RT (Fadouloglou et al., 2000), and then submerged in Amersham™ Amplify™ fluorographic reagent (GE Healthcare) for 30 min at RT to infuse the gel with the fluorographic reagent. PAGE gels were dried completely under vacuum at 80 °C for 2 h. PAGE separated $^{[35]}$S-cysteine labeled products were imaged using BIOMAX MR High-Resolution Film (Carestream).

Immunoprecipitation

Immunoprecipitation (IP) pull-down assays were completed with the use of the magnetic DYKDDDDK (FLAG) immunoprecipitation kit (ClonTech), provided with pre-crosslinked antibody to magnetic beads, per manufacturer's instructions, with one exception. Anti-DYKDDDDK magnetic beads were pre-absorbed by suspending 20 μl beads into 1 ml ClonTech IP lysis buffer supplemented with 0.1% BSA and allowed to tumble at 4 °C overnight prior to the addition of translation products. Approximately 100,000 counts per translation product were then added to the pre-absorbed anti-DYKDDDDK beads suspended in 0.1%BSA/ IP lysis buffer and tumbled for an additional night at 4 °C. Beads were then washed 3 times with ClonTech IP wash buffer per manufacturer's instructions. Washed IP reactions were eluted with the ClonTech IP elution buffer at RT for 5 min. IP beads were removed from eluted products prior to analysis by PAGE under reducing and denaturing conditions.

Isolation of the microsomal fraction

Approximately 250,000 counts per translation reaction were diluted with chilled (4 °C) PBS or tris-buffered sucrose (TBSS buffer; 25 mM Tris–HCl pH7.5, 250 mM sucrose) (Faaberg and Plagemann, 1995). Reactions were diluted to a final volume of 10 ml and mixed thoroughly by gently pipetting. Diluted translation products were stabilized at 4 °C for ≥1 h, followed by pelleting at 150,000*g*, 4 °C, for 1 h. Supernatants from high-speed pelleting were discarded and the resulting pellets were eluted in low volumes (15–25 ul) of chilled PBS or TBSS buffer while keeping all components on ice.

Protease protection assay

Expression constructs and controls were translated as described above, either with or without the addition of canine pancreatic microsomal membranes. Translated products were processed to isolate the microsomal fraction (as described above) using TBSS buffer. Pelleted products were eluted in TBSS buffer and were stabilized at 4 °C for ≥1 h. Stabilized products (4 °C) were then treated with proteinase K (Ambion) (0.6 mg/ml) for 2 h followed by proteinase K inactivation with fresh phenylmethylsulfonyl fluoride (PMSF) (10 mM final concentration) and incubated at 4 °C overnight. Protease protection assay (PPA) reactions were assessed by IP and PAGE analysis as described above.

Acknowledgments

Funding, wholly or in part, was provided by The National Pork Board (#13-196), Boehringer Ingelheim Vetmedica, Inc. (Grant number 991-3625-791), and Project 3625-32000-108-00D of the USDA. USDA is an equal opportunity provider and employer.

References

Abell, B.M., Jung, M., Oliver, J.D., Knight, B.C., Tyedmers, J., Zimmermann, R., High, S., 2003. Tail-anchored and signal-anchored proteins utilize overlapping pathways during membrane insertion. J. Biol. Chem. 278, 5669–5678.

Abell, B.M., Pool, M.R., Schlenker, O., Sinning, I., High, S., 2004. Signal recognition particle mediates post-translational targeting in eukaryotes. EMBO J. 23, 2755–2764.
Abell, B.M., Rabu, C., Leznicki, P., Young, J.C., High, S., 2007. Post-translational integration of tail-anchored proteins is facilitated by defined molecular chaperones. J. Cell Sci. 120, 1743–1751.
Baker, S.C., Baric, R.S., Balasuriya, U.B., Brinton, M.A., Bonami, J.R., Crowley, J.A., de Groot, R.J., Enjuanes, L., Faaberg, K.S., Flegel, T.W., Gorbalenya, A.E., Holmes, K.V., Leung, F.C-C., Lightner, D.V., Nauwynck, H., Perlman, S., Poon, L., Rottier, P.J.M., Snijder, E.J., Stadejk, T., Talbot, P.J., Walker, R.M., Woo, P.C.Y., Yang, H., Yoo, D., Ziebuhr, J., 2012. Nidovirales, In Virus Taxonomy: Ninth Report of the International Committee on Taxonomy of Viruses. Elsevier, London, pp. 785–834.
Bernsel, A., Viklund, H., Falk, J., Lindahl, E., von Heijne, G., Elofsson, A., 2008. Prediction of membrane-protein topology from first principles. Proc. Natl. Acad. Sci. USA 105, 7177–7181.
Bernsel, A., Viklund, H., Hennerdal, A., Elofsson, A., 2009. TOPCONS: consensus prediction of membrane protein topology. Nucleic Acids Res. 37, W465–468.
Brambillasca, S., Yabal, M., Makarow, M., Borgese, N., 2006. Unassisted translocation of large polypeptide domains across phospholipid bilayers. J. Cell Biol. 175, 767–777.
Brambillasca, S., Yabal, M., Soffientini, P., Stefanovic, S., Makarow, M., Hegde, R.S., Borgese, N., 2005. Transmembrane topogenesis of a tail-anchored protein is modulated by membrane lipid composition. EMBO J. 24, 2533–2542.
Corduan, A., Lecomte, S., Martin, C., Michel, D., Desmots, F., 2009. Sequential interplay between BAG6 and HSP70 upon heat shock. Cell. Mol. Life Sci. 66, 1998–2004.
Deaton, M.K., Spear, A., Faaberg, K.S., Pegan, S.D., 2014. The vOTU domain of highly-pathogenic porcine reproductive and respiratory syndrome virus displays a differential substrate preference. Virology 454 – 455, 247–253.
Delgui, L.R., Rodriguez, J.F., Colombo, M.I., 2013. The endosomal pathway and the Golgi complex are involved in the infectious bursal disease virus life cycle. J. Virol. 87, 8993–9007.
Faaberg, K.S., Plagemann, P.G., 1995. The envelope proteins of lactate dehydrogenase-elevating virus and their membrane topography. Virology 212, 512–525.
Fadouloglou, V.E., Glykos, N.M., Kokkinidis, M., 2000. A fast and inexpensive procedure for drying polyacrylamide gels. Anal. Biochem. 287, 185–186.
Fang, Y., Fang, L., Wang, Y., Lei, Y., Luo, R., Wang, D., Chen, H., Xiao, S., 2012a. Porcine reproductive and respiratory syndrome virus nonstructural protein 2 contributes to NF-kappaB activation. Virol. J. 9, 83.
Fang, Y., Snijder, E.J., 2010. The PRRSV replicase: exploring the multifunctionality of an intriguing set of nonstructural proteins. Virus Res. 154, 61–76.
Fang, Y., Treffers, E.E., Li, Y., Tas, A., Sun, Z., van der Meer, Y., de Ru, A.H., van Veelen, P.A., Atkins, J.F., Snijder, E.J., Firth, A.E., 2012b. Efficient -2 frameshifting by mammalian ribosomes to synthesize an additional arterivirus protein. Proc. Natl. Acad. Sci. USA 109, E2920–2928.
Frias-Staheli, N., Giannakopoulos, N.V., Kikkert, M., Taylor, S.L., Bridgen, A., Paragas, J., Richt, J.A., Rowland, R.R., Schmaljohn, C.S., Lenschow, D.J., Snijder, E.J., Garcia-Sastre, A., Virgin, H.W.t., 2007. Ovarian tumor domain-containing viral proteases evade ubiquitin- and ISG15-dependent innate immune responses. Cell Host Microbe 2, 404–416.
Gant Jr., V.U., Moreno, S., Varela-Ramirez, A., Johnson, K.L., 2014. Two membrane-associated regions within the Nodamura virus RNA-dependent RNA polymerase are critical for both mitochondrial localization and RNA replication. J. Virol. 88, 5912–5926.
Gillespie, L.K., Hoenen, A., Morgan, G., Mackenzie, J.M., 2010. The endoplasmic reticulum provides the membrane platform for biogenesis of the flavivirus replication complex. J. Virol. 84, 10438–10447.
Han, J., Rutherford, M.S., Faaberg, K.S., 2009. The porcine reproductive and respiratory syndrome virus nsp2 cysteine protease domain possesses both trans- and cis-cleavage activities. J. Virol. 83, 9449–9463.
Han, J., Rutherford, M.S., Faaberg, K.S., 2010. Proteolytic products of the porcine reproductive and respiratory syndrome virus nsp2 replicase protein. J. Virol. 84, 10102–10112.
Hessa, T., Sharma, A., Mariappan, M., Eshleman, H.D., Gutierrez, E., Hegde, R.S., 2011. Protein targeting and degradation are coupled for elimination of mislocalized proteins. Nature 475, 394–397.
Hsu, N.Y., Ilnytska, O., Belov, G., Santiana, M., Chen, Y.H., Takvorian, P.M., Pau, C., van der Schaar, H., Kaushik-Basu, N., Balla, T., Cameron, C.E., Ehrenfeld, E., van Kuppeveld, F.J., Altan-Bonnet, N., 2010. Viral reorganization of the secretory pathway generates distinct organelles for RNA replication. Cell 141, 799–811.
Kall, L., Krogh, A., Sonnhammer, E.L., 2004. A combined transmembrane topology and signal peptide prediction method. J. Mol. Biol. 338, 1027–1036.
Kang, S.W., Rane, N.S., Kim, S.J., Garrison, J.L., Taunton, J., Hegde, R.S., 2006. Substrate-specific translocational attenuation during ER stress defines a pre-emptive quality control pathway. Cell 127, 999–1013.
Kappes, M.A., Miller, C.L., Faaberg, K.S., 2013. Highly divergent strains of porcine reproductive and respiratory syndrome virus incorporate multiple isoforms of nonstructural protein 2 into virions. J. Virol. 87, 13456–13465.
Knoops, K., Barcena, M., Limpens, R.W., Koster, A.J., Mommaas, A.M., Snijder, E.J., 2012. Ultrastructural characterization of arterivirus replication structures: reshaping the endoplasmic reticulum to accommodate viral RNA synthesis. J. Virol. 86, 2474–2487.
Lambert, C., Prange, R., 2003. Chaperone action in the posttranslational topological reorientation of the hepatitis B virus large envelope protein: implications for translocational regulation. Proc. Natl. Acad. Sci. USA 100, 5199–5204.
Lee, J.G., Ye, Y., 2013. Bag6/Bat3/Scythe: a novel chaperone activity with diverse regulatory functions in protein biogenesis and degradation. Bioessays 35, 377–385.
Leznicki, P., Clancy, A., Schwappach, B., High, S., 2010. Bat3 promotes the membrane integration of tail-anchored proteins. J. Cell Sci. 123, 2170–2178.
Leznicki, P., Roebuck, Q.P., Wunderley, L., Clancy, A., Krysztofinska, E.M., Isaacson, R. L., Warwicker, J., Schwappach, B., High, S., 2013. The association of BAG6 with SGTA and tail-anchored proteins. PLoS One 8, e59590.
Li, Y., Tas, A., Snijder, E.J., Fang, Y., 2012. Identification of porcine reproductive and respiratory syndrome virus ORF1a-encoded non-structural proteins in virus-infected cells. J. Gen. Virol. 93, 829–839.
Li, Y., Treffers, E.E., Napthine, S., Tas, A., Zhu, L., Sun, Z., Bell, S., Mark, B.L., van Veelen, P.A., van Hemert, M.J., Firth, A.E., Brierley, I., Snijder, E.J., Fang, Y., 2014. Transactivation of programmed ribosomal frameshifting by a viral protein. Proc. Natl. Acad. Sci. USA 111, E2172–E2181.
Lu, Y., Turnbull, I.R., Bragin, A., Carveth, K., Verkman, A.S., Skach, W.R., 2000. Reorientation of aquaporin-1 topology during maturation in the endoplasmic reticulum. Mol. Biol. Cell 11, 2973–2985.
Magliano, D., Marshall, J.A., Bowden, D.S., Vardaxis, N., Meanger, J., Lee, J.Y., 1998. Rubella virus replication complexes are virus-modified lysosomes. Virology 240, 57–63.
Mariappan, M., Li, X., Stefanovic, S., Sharma, A., Mateja, A., Keenan, R.J., Hegde, R.S., 2010. A ribosome-associating factor chaperones tail-anchored membrane proteins. Nature 466, 1120–1124.
Miller, D.J., Schwartz, M.D., Ahlquist, P., 2001. Flock house virus RNA replicates on outer mitochondrial membranes in Drosophila cells. J. Virol. 75, 11664–11676.
Nagai, K., Oubridge, C., Kuglstatter, A., Menichelli, E., Isel, C., Jovine, L., 2003. Structure, function and evolution of the signal recognition particle. EMBO J. 22, 3479–3485.
Ota, K., Sakaguchi, M., von Heijne, G., Hamasaki, N., Mihara, K., 1998. Forced transmembrane orientation of hydrophilic polypeptide segments in multi-spanning membrane proteins. Mol. Cell 2, 495–503.
Ott, C.M., Lingappa, V.R., 2004. Signal sequences influence membrane integration of the prion protein. Biochemistry (Moscow) 43, 11973–11982.
Pedersen, K.W., van der Meer, Y., Roos, N., Snijder, E.J., 1999. Open reading frame 1a-encoded subunits of the arterivirus replicase induce endoplasmic reticulum-derived double-membrane vesicles which carry the viral replication complex. J. Virol. 73, 2016–2026.
Rapoport, T.A., 2007. Protein translocation across the eukaryotic endoplasmic reticulum and bacterial plasma membranes. Nature 450, 663–669.
Rapp, M., Granseth, E., Seppala, S., von Heijne, G., 2006. Identification and evolution of dual-topology membrane proteins. Nat. Struct. Mol. Biol. 13, 112–116.
Sasaki, T., Marcon, E., McQuire, T., Arai, Y., Moens, P.B., Okada, H., 2008. Bat3 deficiency accelerates the degradation of Hsp70-2/HspA2 during spermatogenesis. J. Cell Biol. 182, 449–458.
Seppala, S., Slusky, J.S., Lloris-Garcera, P., Rapp, M., von Heijne, G., 2010. Control of membrane protein topology by a single C-terminal residue. Science 328, 1698–1700.
Shen, H., Chou, J.J., 2008. MemBrain: improving the accuracy of predicting transmembrane helices. PLoS One 3, e2399.
Skach, W.R., Calayag, M.C., Lingappa, V.R., 1993. Evidence for an alternate model of human P-glycoprotein structure and biogenesis. J. Biol. Chem. 268, 6903–6908.
Snijder, E.J., Kikkert, M., Fang, Y., 2013. Arterivirus molecular biology and pathogenesis. J. Gen. Virol. 94, 2141–2163.
Snijder, E.J., van Tol, H., Roos, N., Pedersen, K.W., 2001. Non-structural proteins 2 and 3 interact to modify host cell membranes during the formation of the arterivirus replication complex. J. Gen. Virol. 82, 985–994.
Sun, Z., Li, Y., Ransburgh, R., Snijder, E.J., Fang, Y., 2012. Nonstructural protein 2 of porcine reproductive and respiratory syndrome virus inhibits the antiviral function of interferon-stimulated gene 15. J. Virol. 86, 3839–3850.
Tusnady, G.E., Simon, I., 2001. The HMMTOP transmembrane topology prediction server. Bioinformatics 17, 849–850.
van der Meer, Y., van Tol, H., Locker, J.K., Snijder, E.J., 1998. ORF1a-encoded replicase subunits are involved in the membrane association of the arterivirus replication complex. J. Virol. 72, 6689–6698.
van Geest, M., Lolkema, J.S., 2000. Membrane topology and insertion of membrane proteins: search for topogenic signals. Microbiol. Mol. Biol. Rev. 64, 13–33.
van Kasteren, P.B., Bailey-Elkin, B.A., James, T.W., Ninaber, D.K., Beugeling, C., Khajehpour, M., Snijder, E.J., Mark, B.L., Kikkert, M., 2013. Deubiquitinase function of arterivirus papain-like protease 2 suppresses the innate immune response in infected host cells. Proc. Natl. Acad. Sci. USA 110, E838–847.
van Kasteren, P.B., Beugeling, C., Ninaber, D.K., Frias-Staheli, N., van Boheemen, S., Garcia-Sastre, A., Snijder, E.J., Kikkert, M., 2012. Arterivirus and nairovirus ovarian tumor domain-containing Deubiquitinases target activated RIG-I to control innate immune signaling. J. Virol. 86, 773–785.
Viklund, H., Elofsson, A., 2004. Best alpha-helical transmembrane protein topology predictions are achieved using hidden Markov models and evolutionary information. Protein Sci. 13, 1908–1917.
Viklund, H., Elofsson, A., 2008. OCTOPUS: improving topology prediction by two-track ANN-based preference scores and an extended topological grammar. Bioinformatics 24, 1662–1668.
von Heijne, G., 1985. Signal sequences. The limits of variation. J. Mol. Biol. 184, 99–105.
von Heijne, G., 2006. Membrane-protein topology. Nat. Rev. Mol. Cell Biol. 7, 909–918.
von Heijne, G., 2011. Membrane proteins: from bench to bits. Biochem. Soc. Trans. 39, 747–750.

von Heijne, G., Gavel, Y., 1988. Topogenic signals in integral membrane proteins. Eur. J. Biochem. 174, 671–678.
Walter, P., Johnson, A.E., 1994. Signal sequence recognition and protein targeting to the endoplasmic reticulum membrane. Annu. Rev. Cell Biol. 10, 87–119.
Wang, L., Zhou, L., Zhang, H., Li, Y., Ge, X., Guo, X., Yu, K., Yang, H., 2014. Interactome profile of the host cellular proteins and the nonstructural protein 2 of porcine reproductive and respiratory syndrome virus. PLoS One 9, e99176.
Wang, Q., Liu, Y., Soetandyo, N., Baek, K., Hegde, R., Ye, Y., 2011. A ubiquitin ligase-associated chaperone holdase maintains polypeptides in soluble states for proteasome degradation. Mol. Cell 42, 758–770.
Wassenaar, A.L., Spaan, W.J., Gorbalenya, A.E., Snijder, E.J., 1997. Alternative proteolytic processing of the arterivirus replicase ORF1a polyprotein: evidence that NSP2 acts as a cofactor for the NSP4 serine protease. J. Virol. 71, 9313–9322.
Wei, T., Huang, T.S., McNeil, J., Laliberte, J.F., Hong, J., Nelson, R.S., Wang, A., 2010. Sequential recruitment of the endoplasmic reticulum and chloroplasts for plant potyvirus replication. J. Virol. 84, 799–809.
White, S.H., von Heijne, G., 2008. How translocons select transmembrane helices. Annu. Rev. Biophys. 37, 23–42.
Zhang, J.T., Ling, V., 1991. Study of membrane orientation and glycosylated extracellular loops of mouse P-glycoprotein by in vitro translation. J. Biol. Chem. 266, 18224–18232.
Ziebuhr, J., Snijder, E.J., Gorbalenya, A.E., 2000. Virus-encoded proteinases and proteolytic processing in the Nidovirales. J. Gen. Virol. 81, 853–879.